Applied Catalysis B: Environmental 125 (2012) 418–424

Contents lists available at SciVerse ScienceDirect

Applied Catalysis B: Environmental

journal homepage: www.elsevier.com/locate/apcatb

Enhanced Fenton degradation of Rhodamine B over nanoscaled Cu-doped $LaTiO_3$ perovskite

Lili Zhang, Yulun Nie*, Chun Hu*, Jiuhui Qu

State Key Laboratory of Environmental Aquatic Chemistry, Research Center for Eco-Environmental Sciences, Chinese Academy of Sciences, Beijing 100085, China

ARTICLE INFO

Article history:
Received 18 April 2012
Received in revised form 11 June 2012
Accepted 18 June 2012
Available online 23 June 2012

Keywords:
Cu-doped $LaTiO_3$ perovskite
Fenton-like
Active radicals
Rhodamine B

ABSTRACT

Cu-doped $LaTiO_3$ perovskite was prepared with a sol–gel method and characterized by X-ray diffraction and X-ray photoelectron spectroscopy. The introduction of Cu induced the formation of $LaTiO_3$ perovskite in which titanium existed as Ti^{3+}, resulting in the coexistence of $Ti^{3+/4+}$ and $Cu^{+/2+}$ in the perovskite structure. $LaTi_{0.4}Cu_{0.6}O_3$ showed highly Fenton activity and stability for the degradation of RhB with H_2O_2 in the initial pH range of 4–9. Moreover, the catalyst buffered the solution with the tested initial pH to around 7 during the adsorption process. The studies of electron spin resonance, the effect of radical scavengers and other experiments verified that H_2O_2 was predominately converted into $^{\bullet}OH$ and $HO_2^{\bullet}/O_2^{\bullet-}$ in $LaTi_{0.4}Cu_{0.6}O_3$ suspension. A mechanism of heterogeneous Fenton catalysis was proposed on the basis of the both cycles of Ti^{3+}/Ti^{4+} and Cu^{+}/Cu^{2+} during the interaction of $LaTi_{0.4}Cu_{0.6}O_3$ with H_2O_2.

1. Introduction

Advanced oxidation technologies for wastewater treatment have attracted great attention due to the generation of highly potent chemical species ($^{\bullet}OH$, $O_2^{\bullet-}$, etc.), while hydrogen peroxide is a more desirable oxidant agent. The classic Fenton process (dissolved Fe(II) and H_2O_2) [1] is capable of degrading organic pollutants into harmless chemicals such as CO_2 and H_2O, but its application is limited by the narrow working pH range (<4) [2,3], separation and recovery of the iron species specially in industrial wastewater treatment [4]. For these reasons, the development of heterogeneous Fenton systems has received considerable interest and many heterogeneous Fenton-like catalysts have been reported, such as iron oxides [5–8], iron-immobilized zeolites [9], clays [10,11], and carbon materials [12]. Unlike the homogeneous systems, these solid catalysts could be recuperated by means of a simple separation operation and reused in next runs. However, the better catalytic performance is dependent on the presence of ultrasonic and/or UV light irradiation to accelerate the electron transfer at the interface of catalyst and water. Thus, some efforts have been made to develop better heterogeneous Fenton-like catalysts under natural conditions. For example, Na-OL-1 [13] and $BiFeO_3$ [14] have evidenced high catalytic activity in presence of H_2O_2 for the removal of refractory dyes.

On the other hand, the use of low-valency transition-metal ions like Cu^{+} and Ti^{3+} in presence of H_2O_2 may extend the scope of the Fenton reaction. The systems of Cu^{+}-H_2O_2 [15] and Ti^{3+}-H_2O_2 [16] have been found to produce highly potent chemical species, but they require operation under strong acidic conditions to prevent the ion precipitation. If Cu^{+} and Ti^{3+} exist in the solid catalysts, these drawbacks could be overcome. As we know, perovskite-type catalysts (ABO_3) have attracted a great interest for the unique structural features [17,18]: (1) the defined structure, which allows the introduction of various metal ions to its structural framework; (2) the cation at both A- and B-site could be substituted by a foreign one without destroying the matrix structure, which allows the controlled alternation of the oxidation state of cations or the creation of oxygen vacancies. This paper intends to investigate the performance of Cu- and Ti-containing perovskites for wastewater treatment through Fenton-like oxidation.

In this paper, Cu-doped $LaTiO_3$ perovskite was prepared, characterized, and assessed for Fenton catalysis. $LaTi_{0.4}Cu_{0.6}O_3$ was found to be highly effective for the degradation of Rhodamine B (RhB) at wide pH and exhibited excellent long-term stability in the presence of H_2O_2. The possible catalytic mechanism was also discussed.

2. Experimental

2.1. Reagents

Rhodamine B (RhB), lanthanum nitrate ($La(NO_3)_3{\cdot}6H_2O$), copper nitrate trihydrate ($Cu(NO_3)_2{\cdot}3H_2O$), isopropyl alcohol and H_2O_2 (30%, w/w) were purchased from Sinopharm Chemical Reagent Co., Ltd. Tetrabutyl titanate and citric acid were obtained from Beijing Chemical. The reagent *t*-butanol was provided by Tianjin Fuchen Company. 5,5-Dimethyl-1-pyrroline-N-oxide (DMPO),

* Corresponding authors. Tel.: +86 10 62849628; fax: +86 10 62923541.
E-mail addresses: ylnie@rcees.ac.cn (Y. Nie), huchun@rcees.ac.cn (C. Hu).

0926-3373/$ – see front matter © 2012 Elsevier B.V. All rights reserved.
http://dx.doi.org/10.1016/j.apcatb.2012.06.015

N,N-diethyl-p-phenylenediamine sulfate (DPD) and horseradish peroxidase (POD) was supplied by Sigma. For the adjustment of pH, a diluted aqueous solution of nitric acid or sodium hydroxide was employed. All chemicals were at least analytical grade. Deionized water was used throughout this study.

2.2. Catalyst preparation

Cu-doped $LaTiO_3$ perovskite ($LaTi_{1-x}Cu_xO_3$, $x = 0.0–1.0$) was prepared via a preciously reported sol–gel method [19]. In a typical procedure, a mixed solution of $La(NO_3)_3{\cdot}6H_2O$ and $Cu(NO_3)_2{\cdot}3H_2O$ was stirred for 1 h at 0 °C. Thereafter, a tetrabutyl titanate solution in isopropyl alcohol was slowly added. The stoichiometric amount of citric acid was added to form the corresponding metal complexes. After stirring continuously for 2 h, the final solution was heated up to 70 °C to evaporate water. The gel precursor was dried at 110 °C for 24 h and then calcined in air at 700 °C for 5 h. For the highest catalytic activity, the catalyst $LaTi_{0.4}Cu_{0.6}O_3$ was used for all of the experiments unless otherwise specified.

2.3. Characterization

The powder X-ray diffraction (XRD) pattern of the catalyst was recorded on a Scintag-XDS-2000 diffractometer with Cu Kα radiation (λ = 1.540598 Å). The generator voltage and tube current used were 40 kV and 40 mA, respectively. The 2θ ranged from 20° to 70°. The crystalline size was estimated via the Scherer equation. Nitrogen adsorption/desorption experiment was carried out using a Micromeritics ASAP2000 analyzer (Micromeritics, Norcross, GA).

The X-ray photoelectron spectroscopy (XPS) data were taken on an AXIS-Ultra instrument from Kratos using monochromatic Al Kα radiation (225 W, 15 mA, 15 kV) and low-energy electron flooding for charge compensation. To compensate for surface charge effects, the binding energies were calibrated using the C1s hydrocarbon peak at 284.80 eV.

Reactive oxygen species were detected by electron spin resonance (ESR) spectroscopy using DMPO as a spin trap agent. The ESR spectra were obtained using a Bruker model ESP 300E electron paramagnetic resonance spectrometer (center field: 3480.00 G; microwave frequency: 9.79 GHz; and power: 5.05 mW).

2.4. Procedures and analysis

Unless indicated otherwise, 0.07 g catalyst powders were dispersed in 50 mL RhB solution (8 mg L^{-1}). The solution pH was not controlled during the catalytic reaction. Prior to the addition of H_2O_2, the suspensions were magnetically stirred for about 20 min to establish the adsorption/desorption equilibrium between the dye and catalyst. Then, a certain amount of H_2O_2 was added to the above suspensions under continuous magnetic stirring. At given time intervals, 4 mL aliquots were collected and immediately centrifuged to remove the catalyst for analysis. The RhB concentration in the supernatant was determined by recording variations at the wavelength of maximum absorption using a Hitachi UV-3010 UV–visible spectrophotometer. The total organic carbon (TOC) of the solution was analyzed by a Phoenix 8000 analyser (Tekmar-Dohrmann, USA).

To test the stability and recyclability of $LaTi_{0.4}Cu_{0.6}O_3$, the catalyst was filtered, washed with water, and dried at 70 °C. The catalyst was continued to be used in the second cycle. This process was repeated several times.

H_2O_2 concentration was determined using a DPD method described in the literature [20]. The concentrations of La, Ti and Cu in the solutions after reaction for 2 h were measured by inductively coupled plasma optical emission spectrometry (ICP-OES) on an Optima 2000 (PerkinElmer, Inc.) instrument.

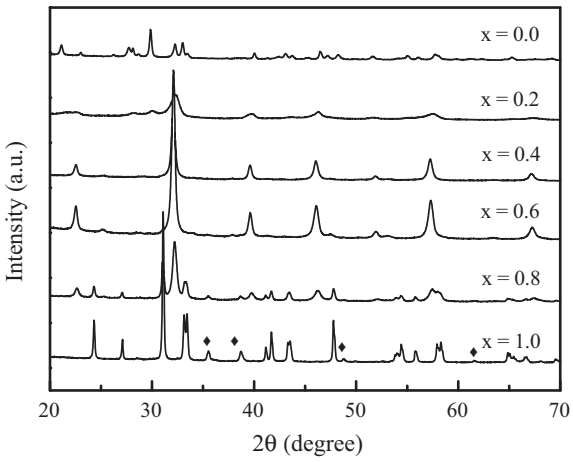

Fig. 1. XRD patterns of the $LaTi_{1-x}Cu_xO_3$ powders.

The experiment data represented the average of the triplicates with a standard deviation less than 5%.

3. Results and discussion

3.1. Characterization of catalysts

A series of Cu-doped $LaTi_{1-x}Cu_xO_3$ ($x = 0.0–1.0$) was synthesized with a sol–gel method. Fig. 1 illustrated XRD patterns of the synthesized samples. All the characteristic peaks of the sample $X_{Cu} = 0$ were well assigned to $La_2Ti_2O_7$ (JCPDS 81-1066). When Cu was introduced, the $La_2Ti_2O_7$ phase disappeared and a $LaTiO_3$ perovskite phase (JCPDS 75-0267) appeared. With an increase of Cu content from $X_{Cu} = 0.2$ to $X_{Cu} = 0.6$, the predominant peaks gradually became stronger and sharper, indicating an increase in the crystallinity of $LaTiO_3$ phase. The addition of excessive Cu ($X_{Cu} = 0.8$) in the preparation process resulted in the appearence of the impurities La_2CuO_4 (JCPDS 82-2142) and CuO (JCPDS 48-1548). In addition, the main phase of the sample $X_{Cu} = 1.0$ became La_2CuO_4 with a few CuO (♦). It can be seen that a phase transition process occurred with an increase of Cu content. According to the XRD results, the introduction of Cu induced the formation of the crystalline phase $LaTiO_3$ in which titanium existed as Ti^{3+} [21]. The average size of $LaTi_{0.4}Cu_{0.6}O_3$ crystallite was 38.2 nm based on the calculation with Scherer equation. The BET surface area was 8.5 $m^2\,g^{-1}$.

In order to confirm the oxidation states of the surface metal species, XPS measurements were conducted on the samples $X_{Cu} = 0.0$ and $X_{Cu} = 0.6$. According to the XPS data, the La 3d peaks of both samples appeared at 834.1 eV ($3d_{5/2}$) and 850.7 eV ($3d_{3/2}$) which corresponded to La^{3+}. As shown in Fig. 2, the strong peak at 458.0 eV could be assigned to Ti^{4+} [22,23] for the sample $X_{Cu} = 0.0$, while the Ti $2p_{3/2}$ peak of the sample $X_{Cu} = 0.6$ was well fit into the peaks of Ti^{3+} (~457.5 eV) and Ti^{4+} (~458.5 eV) [24] and the surface concentration ratio of Ti^{3+} to Ti^{4+} was about 4.6:1. Therefore, it was confirmed that the insertion of Cu into the La/Ti system led to the conversion of the crystalline phase from $La_2Ti_2O_7$ to $LaTiO_3$, thus produced the existence environment of the Ti^{3+} ion which could exhibit higher Fenton catalytic activity. In the Cu 2p core level spectra of the sample $X_{Cu} = 0.6$, the peaks corresponding to Cu $2p_{3/2}$ were observed at ca. 932.6 and 934.2 eV for reduced copper species and Cu^{2+}, respectively [25]. Cu^{2+} ion could also be distinguished by the appearance of a shake-up satellite line at ca. 940.0–942.6 eV. The identification of the reduced copper species, i.e., Cu^0 and/or Cu^+, became extremely difficult by XPS data alone since the BE for Cu^0 and Cu^+ were almost the same [26]. Therefore, AES measurements

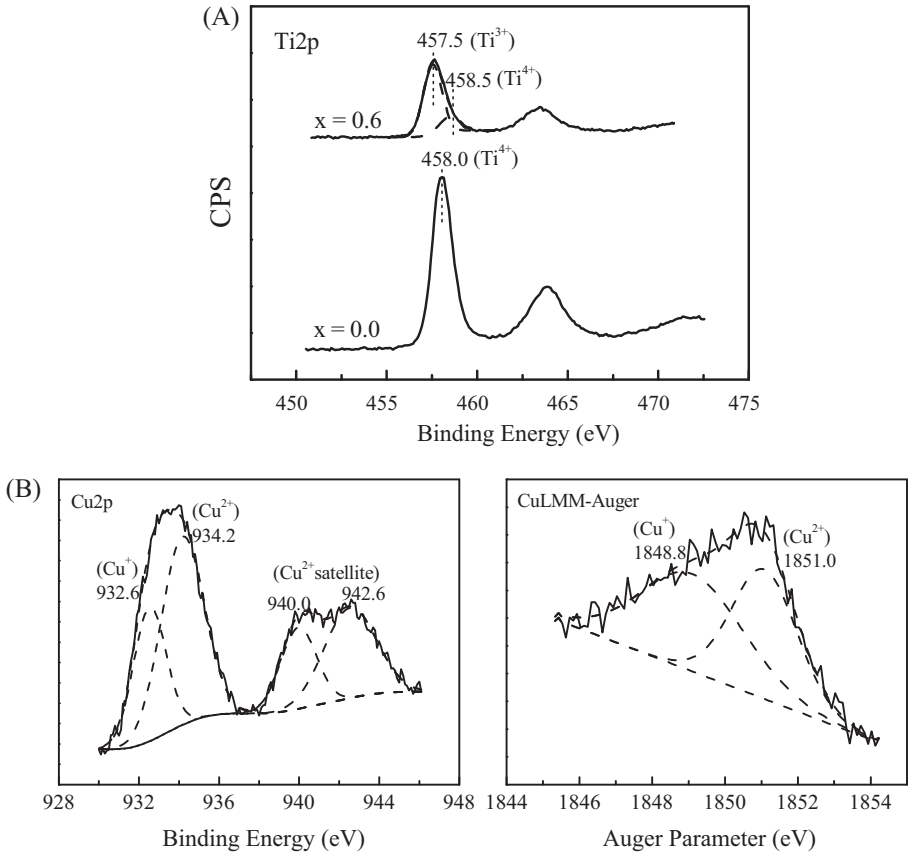

Fig. 2. XPS spectra of the $LaTi_{1-x}Cu_xO_3$ powders: (A) Ti2p; (B) Cu2p (left) and LMM X-ray induced Auger parameter (right) for the sample $x = 0.6$.

were performed. The auger parameters at 1848.8 eV and 1851.0 eV confirmed the existence of Cu^+ and Cu^{2+}, respectively. The concentration ratio of Cu^+ to Cu^{2+} on the surface of the catalyst was about 0.28:1.

3.2. Catalytic activity and stability of $LaTi_{0.4}Cu_{0.6}O_3$

The Fenton catalytic activity of $LaTi_{1-x}Cu_xO_3$ was evaluated by the oxidation of RhB in aqueous solution with H_2O_2. As shown in Fig. 3, no significant decolorization was observed in the presence of the sample $X_{Cu} = 0$ ($La_2Ti_2O_7$), while the introduction of

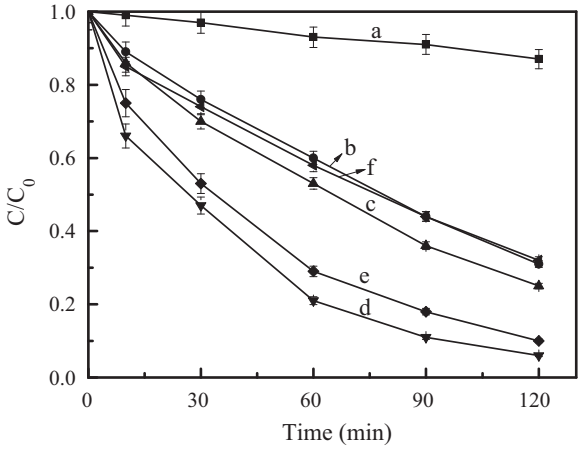

Fig. 3. Fenton-like degradation of RhB (8 mg L^{-1}) in the presence of $LaTi_{1-x}Cu_xO_3$ suspensions (1.4 g L^{-1}) and H_2O_2 (20 mM): (a) $x = 0.0$; (b) $x = 0.2$; (c) $x = 0.4$; (d) $x = 0.6$; (e) $x = 0.8$; and (f) $x = 1.0$.

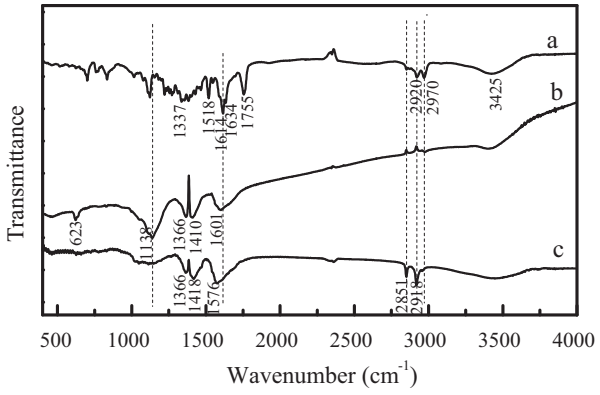

Fig. 4. Changes of FT-IR spectra during the degradation of RhB (8 mg L^{-1}) in $LaTi_{0.4}Cu_{0.6}O_3$ (1.4 g L^{-1}) suspensions with H_2O_2 (20 mM) at different reaction times: (a) 0 min; (b) 120 min; and (c) 180 min.

Cu strongly increased Fenton catalytic activity of the oxides. The decolorization rate of RhB increased with increasing Cu content in the catalysts from $X_{Cu} = 0.2$ to $X_{Cu} = 0.6$, but the presence of excessive Cu in the catalysts (i.e. $X_{Cu} = 0.8$ and 1.0) decreased the degradation of RhB. Based on the obtained results, well-crystallized $LaTi_{0.4}Cu_{0.6}O_3$ with a pure $LaTiO_3$ phase had the highest activity. The results indicated that the coexistence of reduced metal ions Ti^{3+} and Cu^+ enhanced Fenton catalytic activity of the catalyst. In $LaTi_{0.4}Cu_{0.6}O_3/H_2O_2$ suspension, about 94% of RhB was decolorized while about 57% of TOC content was removed within 120 min at neutral pH. The FT-IR spectra in Fig. 4 showed the degradation process of RhB in the presence of $LaTi_{0.4}Cu_{0.6}O_3$ and H_2O_2. In curve a, the band at 3425 cm^{-1} was due to —OH stretch vibration, and

the bands at 2970, 2920 cm^{-1} were caused by —CH_2— and C—CH_3 stretch vibrations, respectively [27,28]. The peaks at 1614, 1547, 1518, 1466 cm^{-1} corresponded to aromatic ring vibrations, while the 1337 cm^{-1} peak attributed to C-aryl bond vibration; the peak at 1755 cm^{-1} was due to C=O groups. The peak at 1634 cm^{-1} was caused by the C—N bond vibration and the heterocycle vibrations caused the peaks ranging at 1518–1547 cm^{-1}. As shown in curve b, the peak at 1614 cm^{-1} corresponded to aromatic ring vibrations shifted to 1601 cm^{-1} and other characteristic peaks disappeared after reaction for 120 min. Meanwhile, the new peaks at 1410, 1366, 1138 and 623 cm^{-1} appeared. The results indicated that the disappearance of the parental RhB structure and the generation of its primary aromatic breakdown products. In curve c, after reaction for 180 min, the new strong peaks 1138 and 623 cm^{-1} disappeared, while 2918 and 2851 cm^{-1} for C—H asymmetric/symmetric stretching of —CH_3 and —CH_2— groups appeared. Moreover, the new strong peak at 1030–1148 cm^{-1} was caused by —C—O—H stretch vibration. The results implied the intermediate organic products were further degraded into smaller organic molecules such as alcohols and inorganic species.

The stability and reusability of $LaTi_{0.4}Cu_{0.6}O_3$ was evaluated by RhB degradation. The leaching of La and Cu from the catalyst $LaTi_{0.4}Cu_{0.6}O_3$ during the RhB degradation process was tested by using ICP-OES method. It was found that there was no significant leaching of La and Cu ions at initial pH 9.0 and 6.8 in Fig. S1. At pH 4.0, the concentrations of leached La and Cu were 4.6 mg L^{-1} and 1.4 mg L^{-1}, respectively. In addition, no leaching of Ti was detected at the tested pH. Especially, $LaTi_{0.4}Cu_{0.6}O_3$ was able to be reused for at least six cycles and exhibited no significant loss of activity in Fig. 5. Furthermore, no significant difference was observed in the structure of $LaTi_{0.4}Cu_{0.6}O_3$ between before and after reaction by XRD and XPS measurements as shown in Figs. 6 and 7. The results indicated that the catalyst had an excellent long-term stability.

3.3. Effects of H_2O_2 concentration and initial pH

The effects of H_2O_2 concentration and initial pH on the catalytic activity of $LaTi_{0.4}Cu_{0.6}O_3$ were investigated. As shown in Fig. 8, only 8% of RhB was decolorized without H_2O_2 even after reacting for 120 min. The degradation of RhB was significantly accelerated in the presence of H_2O_2. When 10 mM H_2O_2 was added, about 84% of RhB was decolorized within 120 min. And catalytic decolorization of up to 94% was observed with 20 mM H_2O_2 added. However, H_2O_2 dosage more than 20 mM resulted in a slight increase in the decolorization due to an unprofitable consumption of H_2O_2 from the scavenging effect of H_2O_2. Fig. 9 shows the RhB degradation in $LaTi_{0.4}Cu_{0.6}O_3$ with 20 mM H_2O_2 at different initial pH.

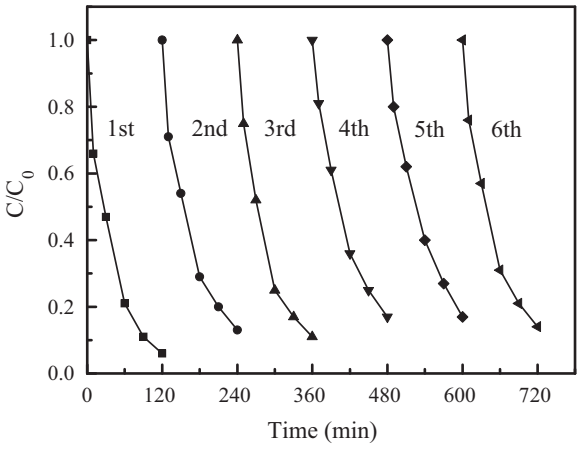

Fig. 5. Stability of the $LaTi_{0.4}Cu_{0.6}O_3$ catalyst for the decolorization of RhB (8 mg L^{-1}).

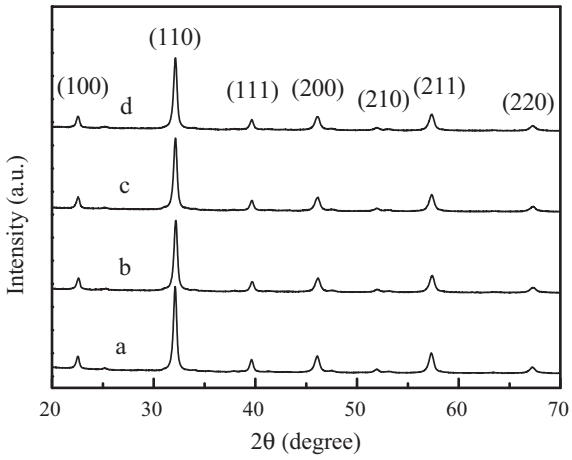

Fig. 6. XRD patterns of the $LaTi_{0.4}Cu_{0.6}O_3$ powders: (a) as-prepared; (b) after the first run; (c) after the second run; and (d) after the third run.

$LaTi_{0.4}Cu_{0.6}O_3$ exhibited a high catalytic activity at initial pH values from 4.0 to 6.8, followed by a slight decrease of RhB decolorization at higher initial pH 9.0. As shown in the inset of Fig. 9, the solution pH gradually tended to be neutral during the adsorption of RhB, then decreased slightly when H_2O_2 was added and finally stabilized during the catalytic reaction. It seemed that the catalyst $LaTi_{0.4}Cu_{0.6}O_3$ had a good acid and alkaline buffer performance, which led to its excellent catalytic ability in a wide pH range.

3.4. Reaction mechanism

To ascertain the reaction mechanism, DMPO spin-trap ESR was performed to detect the reactive oxygen species (ROS) involved in the $LaTi_{0.4}Cu_{0.6}O_3/H_2O_2$ system. As shown in Fig. 10, no significant signals were attributed to ROS in the control experiments in the absence of H_2O_2, while four characteristic peaks of DMPO-•OH were observed in the suspension of $LaTi_{0.4}Cu_{0.6}O_3$ with H_2O_2.

The formation of $HO_2^{\bullet}/O_2^{\bullet-}$ radicals was also detected in methanol (Fig. 10B), since the $HO_2^{\bullet}/O_2^{\bullet-}$ radicals in water were very unstable and underwent facile disproportionation rather than slow reaction with DMPO [29]. The sextet peaks of DMPO-$HO_2^{\bullet}/O_2^{\bullet-}$ adducts were observed in $LaTi_{0.4}Cu_{0.6}O_3$ suspension with H_2O_2. The results indicated H_2O_2 was decomposed into •OH and $HO_2^{\bullet}/O_2^{\bullet-}$ radicals by the redox reaction with $LaTi_{0.4}Cu_{0.6}O_3$.

Furthermore, the effects of radical scavengers on the decolorization rate of RhB were investigated. *t*-Butanol and *p*-benzoquinone [30] were selected as •OH and $HO_2^{\bullet}/O_2^{\bullet-}$ radical scavengers, respectively. The decolorization of RhB was almost completely depressed in the presence of *t*-butanol and only 25% of RhB was decolorized within 120 min, while the addition of *p*-benzoquinone also inhibited the decolorization of RhB in Fig. 11. These results confirmed that both •OH and $HO_2^{\bullet}/O_2^{\bullet-}$ radicals were the active species involved in the process of RhB degradation.

As shown in Fig. 12, the decomposition of H_2O_2 (20 mM) was still incomplete after 20 h reaction in $LaTi_{0.4}Cu_{0.6}O_3$ without organic compounds, and the presence of the substrate RhB decreased the decomposition of H_2O_2. These results suggested that the H_2O_2 decomposition and the RhB oxidation were competitive processes involving the same active species [31], which reacted with H_2O_2 enhancing the decomposition rate, indicating that H_2O_2 was predominantly decomposed into active radicals rather than O_2.

The oxygen vacancy played a fundamental role in reducing H_2O_2 to O_2 [32]. Moreover, there was a considerable amount of oxygen vacancy on the surface of $LaTi_{0.4}Cu_{0.6}O_3$ (Fig. S2 and Table S1), which was calculated from the variation of area ratio of the two O1s peaks according to the reported method [33]. However, the H_2O_2

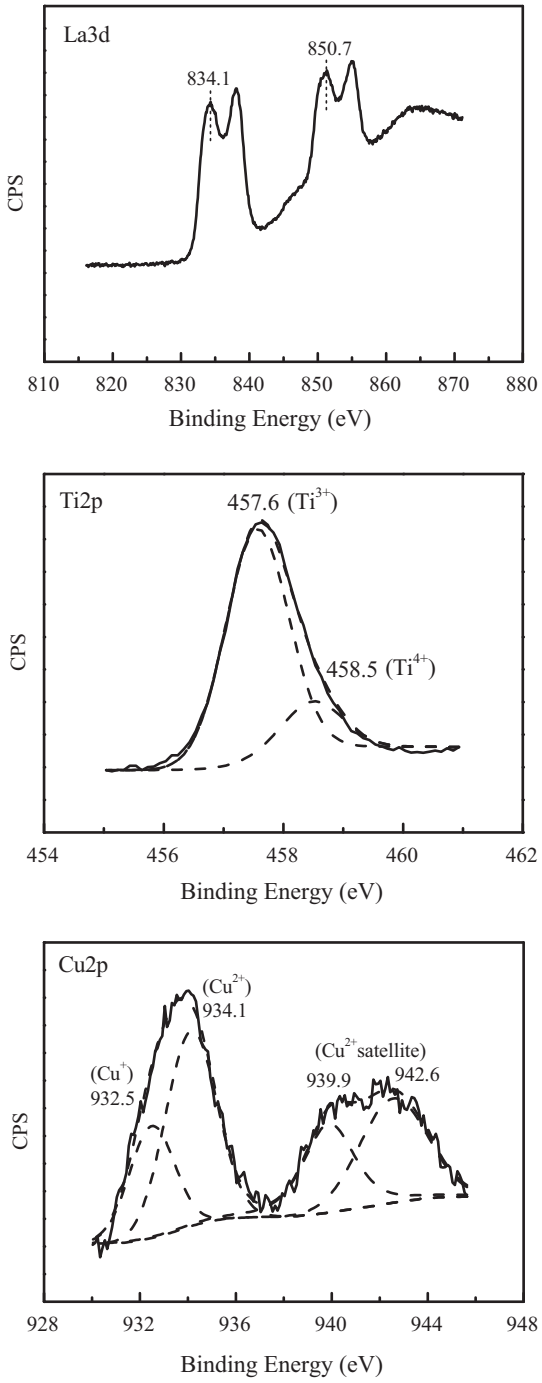

Fig. 7. XPS spectra of the $LaTi_{0.4}Cu_{0.6}O_3$ powders after reaction.

decomposition reaction proceeded via a radical mechanism by the studies of electron spin resonance, the effect of radical scavengers and the H_2O_2 decompositon experiments, indicating that the oxygen vacancy did not influence much on the reaction due to the role of Cu and Ti in the catalyst.

The presence of $Ti^{3+/4+}$ and $Cu^{+/2+}$ on the surface of $LaTi_{0.4}Cu_{0.6}O_3$ was confirmed using the XPS technology. The surface concentration ratio of Ti^{3+} to Ti^{4+} was about 4.6:1 and that of Cu^+ to Cu^{2+} was about 0.28:1 before reaction, while the surface concentration ratio of Ti^{3+} to Ti^{4+} was about 5.1:1 and that of Cu^+ to Cu^{2+} was about 0.23:1 after reaction. There was no significant difference in Ti^{3+}/Ti^{4+} or Cu^+/Cu^{2+} on the surface of catalyst before and after catalytic reaction, suggesting $Cu^+(Ti^{3+})$ participated in the

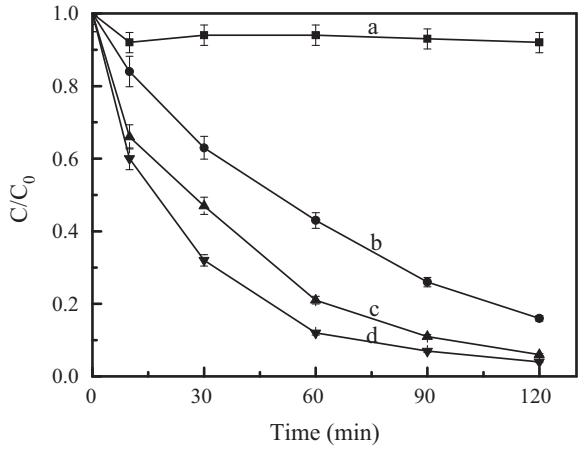

Fig. 8. Effect of initial concentration of H_2O_2 on decolorization of RhB (8 mg L^{-1}) in $LaTi_{0.4}Cu_{0.6}O_3$ (1.4 g L^{-1}) suspensions: (a) 0 mM; (b) 10 mM; (c) 20 mM; and (d) 40 mM.

redox cycle. In addition, ESR and the radical inhibition experiments had confirmed $^{\bullet}OH$ and $HO_2^{\bullet}/O_2^{\bullet-}$ radicals were the active species. These results suggested that an interfacial electron cycle process occurred (Eqs. (1)–(6)) according to the experimental data and a review of the literature [34–37]. A mechanism for ROS formation was proposed as follows:

$$Ti^{3+} + H_2O_2 \rightarrow Ti^{4+} + {}^{\bullet}OH + OH^- \quad (1)$$

$$Cu^{2+} + H_2O_2 \rightarrow Cu^+ \cdot O_2H + H^+ \quad (2)$$

$$Cu^+ \cdot O_2H + H_2O_2 \rightarrow Cu^+ + O_2 + {}^{\bullet}OH + H_2O \quad (3)$$

$$H^+ + Cu^+ + H_2O_2 \rightarrow Cu^{2+} + {}^{\bullet}OH + H_2O \quad (4)$$

$$H_2O_2 + {}^{\bullet}OH \rightarrow H_2O + HO_2^{\bullet} \quad (5)$$

$$Ti^{4+} + HO_2^{\bullet} \rightarrow Ti^{3+} + H^+ + O_2 \quad (6)$$

$$RhB + {}^{\bullet}OH \rightarrow \ldots \rightarrow CO_2 + H_2O \quad (7)$$

Ti^{3+}, as the main surface Ti species, initiated redox cycling to generate OH radicals via the Harber–Weiss reaction (Eq. (1)). Cu^{2+} catalyzed the decomposition of H_2O_2 into OH radicals as Eqs. (2)–(4). Cu^+ was also Fenton active and could participate in radical-generating cycles. The active species might react with H_2O_2 and Ti^{4+} to form O_2 (Eqs. (5) and (6)) or oxidize the organic molecule in aqueous medium (Eq. (7)). The more content of Ti^{4+} in the catalyst was not useful for the degradation of RhB in the Fenton reaction.

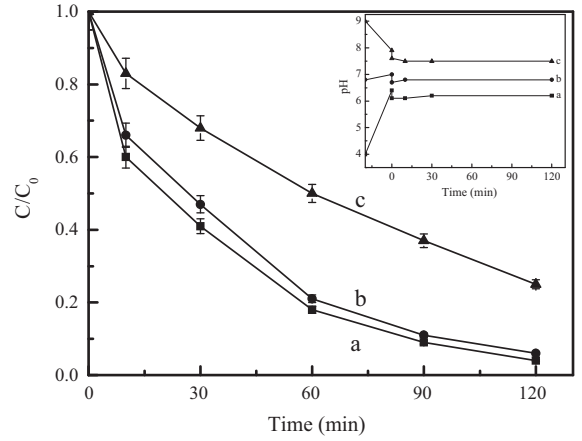

Fig. 9. Effect of initial pH on decolorization of RhB (8 mg L^{-1}) in the presence of $LaTi_{0.4}Cu_{0.6}O_3$ suspensions (1.4 g L^{-1}) and H_2O_2 (20 mM): (a) 4.0; (b) 6.8; and (c) 9.0. The inset indicates the changes of solution pH during reaction.

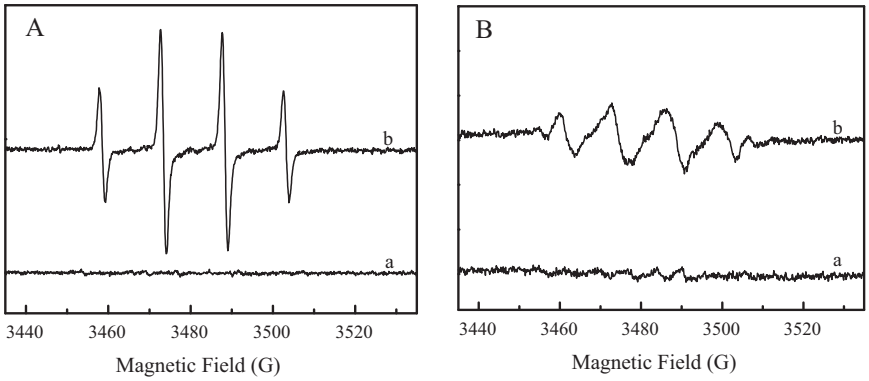

Fig. 10. DMPO spin trapping ESR spectra recorded in the dark at ambient temperature with $LaTi_{0.4}Cu_{0.6}O_3$ as catalyst (A) in aqueous dispersion for DMPO-•OH and (B) in methanol dispersion for DMPO-$HO_2^•/O_2^{•-}$: (a) without and (b) with H_2O_2.

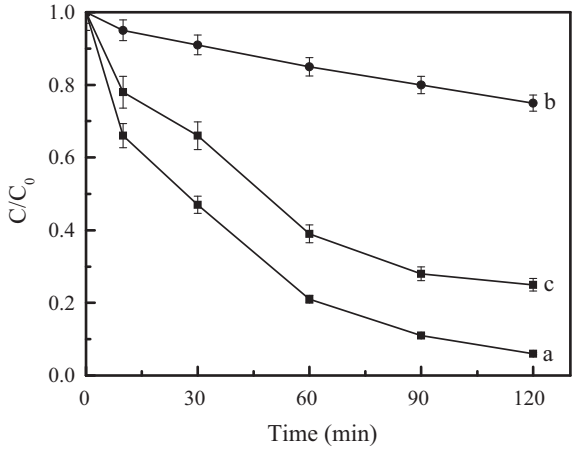

Fig. 11. Decolorization of RhB (8 mg L^{-1}) in the presence of $LaTi_{0.4}Cu_{0.6}O_3$ suspensions (1.4 g L^{-1}) and H_2O_2 (20 mM) with (a) no scavenger added, (b) 10 mM *t*-butanol, and (c) 10 mM *p*-benzoquinone.

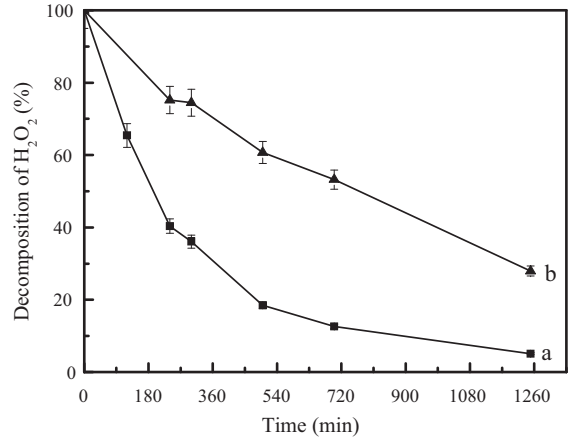

Fig. 12. Decomposition of H_2O_2 in the systems of (a) $LaTi_{0.4}Cu_{0.6}O_3$ (1.4 g L^{-1})–H_2O_2 (20 mM)–H_2O and (b) $LaTi_{0.4}Cu_{0.6}O_3$ (1.4 g L^{-1})–H_2O_2 (20 mM)–RhB (8 mg L^{-1}).

It was also in line with the existence of an optimum value for the H_2O_2 concentration due to the radical scavenging effect of H_2O_2.

4. Conclusions

Nanoscaled Cu-doped $LaTiO_3$ perovskite exhibited high activity and stability for the decolorization and mineralization of RhB with H_2O_2 in the initial pH range of 4–9. •OH and $HO_2^•/O_2^{•-}$ radicals were the main active species in the reaction by the studies of ESR and the radical inhibition effect. The insertion of Cu into the La/Ti system led to the conversion of the crystalline phase from $La_2Ti_2O_7$ to $LaTiO_3$, thus resulting in the existence of Ti^{3+} as the predominant titanium species in the perovskite structure which could exhibit high Fenton catalytic activity. Cu^{2+} could initiate redox cycling to generate active radicals and Cu^+ was also Fenton active to participate in radical-generating cycles. As a whole, the coexistence of $Ti^{3+/4+}$ and $Cu^{+/2+}$ in the perovskite structure greatly enhanced the H_2O_2 decomposition into active radicals, resulting in the high Fenton catalytic activity.

Acknowledgments

This work was supported by the National Natural Science Foundation of China (nos. 50908223, 50921064, and 21125731) and the National 973 Project of China (grant no. 2010CB933600).

Appendix A. Supplementary data

Supplementary data associated with this article can be found, in the online version, at http://dx.doi.org/10.1016/j.apcatb.2012.06.015.

References

[1] F. Haber, J. Weiss, R. Proc, Proceedings of the Royal Society of London Series A 147 (1934) 332–351.
[2] D.L. Sedlak, A.W. Andren, Environmental Science and Technology 25 (1991) 777–782.
[3] J.J. Pignatello, Environmental Science and Technology 26 (1992) 944–951.
[4] S. Parra, I. Guasaquillo, O. Enea, E. Mielczarski, J. Mielczarki, P. Albers, L. Kiwi-Minsker, J. Kiwi, Journal of Physical Chemistry B 107 (2003) 7026–7035.
[5] R.C.C. Costa, M.F.F. Lelis, L.C.A. Oliveira, J.D. Fabris, J.D. Ardisson, R.R.V.A. Rios, C.N. Silva, R.M. Lago, Journal of Hazardous Materials 129 (2006) 171–178.
[6] F. Magalhães, M.C. Pereira, S.E.C. Botrel, J.D. Fabris, W.A. Macedo, R. Mendonça, R.M. Lago, L.C.A. Oliveira, Applied Catalysis A: General 332 (2007) 115–123.
[7] A.C. Silva, D.Q.L. Oliveira, L.C.A. Oliveira, A.S. Anastácio, T.C. Ramalho, J.H. Lopes, H.W.P. Carvalho, C.E.R. Torres, Applied Catalysis A: General 357 (2009) 79–84.
[8] S. Yang, H. He, D. Wu, D. Chen, X. Liang, Z. Qin, M. Fan, J. Zhu, P. Yuan, Applied Catalysis B: Environmental 89 (2009) 527–535.
[9] M.B. Kasiri, H. Aleboyeh, A. Aleboyeh, Applied Catalysis B: Environmental 84 (2008) 9–15.
[10] B. Iurascu, I. Siminiceanu, D. Vione, M.A. Vicente, A. Gil, Water Research 43 (2009) 1313–1322.
[11] G.K. Zhang, Y.Y. Gao, Y.L. Zhang, Y.D. Guo, Environmental Science and Technology 44 (2010) 6384–6389.
[12] F. Duarte, F.J. Maldonado-Hódar, A.F. Pérez-Cadenas, L.M. Madeira, Applied Catalysis B: Environmental 85 (2009) 139–147.
[13] L.L. Zhang, Y.L. Nie, C. Hu, X.X. Hu, Journal of Hazardous Materials 190 (2011) 780–785.
[14] W. Luo, L.H. Zhu, N. Wang, H.Q. Tang, M.J. Cao, Y.B. She, Environmental Science and Technology 44 (2010) 1786–1791.
[15] M.K. Eberhardt, G. Ramirez, E. Ayala, Journal of Organic Chemistry 54 (1989) 5922–5926.

[16] G. Lassmann, L.A. Eriksson, F. Himo, F. Lendzian, W. Lubitz, Journal of Physical Chemistry A 103 (1999) 1283–1290.
[17] R.J.H. Voorhoeve, D.W. Johnson, J.P. Remeika, P.K. Gallagher, Science 195 (1977) 827–833.
[18] J.J. Zhu, A. Thomas, Applied Catalysis B: Environmental 92 (2009) 225–233.
[19] F.J. Beltran, P. Pocostales, P.M. Alvarez, F. Lopez-Pineiro, Applied Catalysis B: Environmental 92 (2009) 262–270.
[20] H. Bader, V. Sturzenegger, J. Hoigne, Water Research 22 (1988) 1109–1115.
[21] A.A. Mozhegorov, A.E. Nikiforov, A.V. Larin, A.V. Efremov, L.E. Gonchar, P.A. Agzamova, Physics of the Solid State 50 (2008) 1795–1798.
[22] Y.A. Teterin, S.V. Stefanovskij, S.V. Yudintsev, G.N. Bek-uzarov, A.Y. Teterin, K.I. Maslakov, I.O. Utkin, Nuclear Technology & Radiation Protection 19 (2004) 31–38.
[23] Y. Masuda, R. Mashima, M. Yamada, K. Ikeuchi, K. Murai, G.I.N. Waterhouse, J.B. Metson, T. Moriga, Journal of the Ceramic Society of Japan 117 (2009) 76–81.
[24] S. Song, J.J. Tu, Z.Q. He, F.Y. Hong, W.P. Liu, J.M. Chen, Applied Catalysis A: General 378 (2010) 169–174.
[25] F.E. Lopez-Suarez, S. Parres-Esclapez, A. Bueno-Lopez, M.J. Illan-Gomez, B. Ura, J. Trawczynski, Applied Catalysis B: Environmental 93 (2009) 82–89.
[26] J.L.G. Fierro, Catalysis Reviews 34 (1992) 321–336.
[27] G. Liu, X. Li, J. Zhao, H. Hidaka, N. Serpone, Environmental Science and Technology 34 (2000) 3982–3990.
[28] J.Y. Li, W.H. Ma, P.X. Lei, J.C. Zhao, Journal of Environmental Science 19 (2007) 892–896.
[29] W.H. Ma, Y.P. Huang, J. Li, M.M. Cheng, W.J. Song, J.C. Zhao, Chemical Communications (2003) 1582–1583.
[30] M.C. Yin, Z.S. Li, J.H. Kou, Z.G. Zou, Environmental Science and Technology 43 (2009) 8361–8366.
[31] R.C.C. Costa, M.d.F.F. Lelis, L.C.A. Oliveira, J.D. Fabris, J.D. Ardisson, R.R.V.A. Rios, C.N. Silva, R.M. Lago, Catalysis Communications 4 (2003) 525–529.
[32] Y.N. Lee, R.M. Lago, J.L.G. Fierro, J. González, Applied Catalysis A: General 215 (2001) 245–256.
[33] W. Cao, O.K. Tan, J.S. Pan, W. Zhua, C.V.G. Reddy, Materials Chemistry and Physics 75 (2002) 67–70.
[34] Y. Ohashi, H. Yoshioka, H. Yoshioka, Bioscience, Biotechnology, and Biochemistry 66 (2002) 847–852.
[35] C. Randorn, S. Wongnawa, P. Boonsin, ScienceAsia 30 (2004) 149–156.
[36] C. Wang, L. Liu, L. Zhang, Y. Peng, F. Zhou, Biochemistry 49 (2010) 8134–8142.
[37] L. Khachatryan, E. Vejerano, S. Lomnicki, B. Dellinger, Environmental Science and Technology 45 (2011) 8559–8566.